Jestr

Journal of Engineering Science and Technology Review 16 (6) (2023) 44 - 53

Research Article

JOURNAL OF
Engineering Science and Technology Review

www.jestr.org

Study on Mechanical Properties of Fiber-reinforced Concrete

Jingjing Zhang[1] , Kaizhao Han[1] , Mengzhao Wang[1], Jianwei Cheng[2,*] and Ruoyang Wu[3]

[1]*School of Architectural Engineering, North China Institute of Aerospace Engineering, Langfang 065000, China*
[2]*Tianjin Wan 'an Jianchuang Real Estate Co., LTD., Tianjin 300380, China*
[3]*Consor Engineers, Plano 75025, USA*

Received 19 September 2023; Accepted 2 December 2023

Abstract

Concrete is a widely used building material. However, due to its inherent shortcomings, such as its susceptibility to cracking and poor toughness, the durability and service life of a structure are greatly affected. To explore the enhancement effects of different fiber types and blends on crack resistance and toughness of concrete, this study presents the models of different kinds of fiber-reinforced concrete (FRC) with different contents. Various combinations of carbon fiber, aramid fiber, and a hybrid fusion of both were simultaneously integrated into concrete using three blends, and the stress – strain curve of FRC was established through axial compression test. The model parameters were analyzed based on three different constitutive models, combined with the test data. On this basis, the finite element model of FRC was established, and the accuracy of the model was verified through test data. Results show that, the compressive strength of concrete with 0.6% fiber content is the highest. The maximum increase rate is approximately 10%, and the fiber hybrid reflects a positive effect. The numerical simulation results of the stress – strain constitutive relationship of FRC under compression decline relatively slowly in the softening section. Comparison between the compressive strength of the model with the test value, the error is less than 15%, thereby affirming the high accuracy of the model. This study provides a significantly reference for the popularization and application of hybrid FRC with carbon and aramid.

Keywords: Mechanical properties, Fiber-reinforced concrete, Compression test, Strength

1. Introduction

Nowadays, concrete has emerged as a pivotal material widely used in constructing structures, primarily owing to its advantages, including high hardness, abundant raw material sources, low cost, easy adaptability in performance, and user friendliness [1]. The application and demand for concrete show a trend of gradual growth, and related study has also made great progress. An increasing number of units are involved in all aspects, namely, study, design, production, and application of concrete [2].

However, with the deepening of study, concrete finds extensive application in many pivotal projects. Scholars found that concrete exhibits low tensile strength, small limit elongation, brittleness, and other deficiencies. The broader the application of concrete is, the more pronounced these problems become, which has a remarkable effects on the use of buildings and later maintenance.

Based on these findings, scholars have conducted many studies on improving the tensile strength and toughness of concrete [3-4]. Fiber exhibits good tensile properties and toughness [5-7]. Results demonstrate that incorporating different types of fiber materials to concrete can effectively overcome its inherent shortcomings [8-9]. Therefore, fiber-reinforced concrete (FRC) has become a research hotspot in recent years. The use and promotion of FRC is also an inevitable trend. However, the diverse array of available fibers presents a challenge due to their varying qualities, and different kinds of fibers have unique properties. At present, problems persist in the study of FRC. Shortcomings are also observed in the properties of fiber itself. For instance, steel fiber and basalt fiber exhibit poor corrosion resistance, wherein steel fiber is heavier. All of the above have some adverse effects on FRC components. The improvement effects and mechanisms of the performance of various fiber types in substrates necessitate further experimental study [10]. Moreover, the influence of fiber content on the mechanical properties of concrete varies.

To this end, this study adopts carbon fiber and aramid fiber with high strength and elastic modulus, corrosion resistance, and high temperature resistance to improve the performance of concrete. The stress – strain curve is drawn by axial compression test. The constitutive model of FRC was established to analyze and compare the effects of different types and fiber addition rates on the performance of concrete. The reference is provided for the performance of concrete mixed with carbon fiber and aramid fiber.

2. State of the art

At present, scholars have extensively investigated the mechanical properties of FRC. Zhang et al. [11] conducted a series of material tests and numerical simulations to investigate the stability of FRC tunnel linings with different crack features under train load. Meanwhile, the compressive properties of FRC had not been analyzed in detail. To study the effects of aggregate size and fiber length on the mechanical properties of basalt FRC, Zhang Xiaofei et al. [12] performed axial compression test, splitting tensile test, and bending test. The influence of the parameters on compressive strength, splitting tensile strength, and flexural strength was analyzed. The finite element modeling analysis

*E-mail address: 15022741875@163.com
ISSN: 1791-2377
doi:10.25103/jestr.166.06

of ABAQUS was conducted by using random fiber script, and the corresponding strength calculation method was proposed. However, the influence factor of fiber content was not deeply analyzed. With regard to the controversy of fiber selection and effect characterization of FRC, Zhao et al. [13] reviewed, summarized, and compared the study status of FRC. However, the compressive properties of FRC had not been studied deeply. Liu et al. [14] conducted experimental and theoretical studies on the incorporation of steel fiber and synthetic fiber into reinforced concrete segments. However, the characterization of the interaction between the two fibers was lacking. Wang et al. [15] studied the load bearing characteristics of basalt FRC lining. Meanwhile, the fiber concrete studied was relatively simple, and no other fiber concrete control groups was set up based on the existing study on the influence of fiber orientation on the mechanical properties of FRC. Li et al. [16] conducted further study on the mechanical properties of oriented distributed steel FRC through splitting tensile and bending tests. However, the influencing factor of fiber content had not been analyzed deeply. Guler et al. [17] investigated the slump, mass loss, wear loss, residual compressive strength, and residual splitting tensile strength of single and mixed FRCs with wollastonite and basalt after freeze–thaw cycles. However, the compression resistance of FRC axis was not described in detail. To investigate the effectiveness of improving fiber matrix to improve the performance of FRC mixture, Onur et al. [18] prepared FRC mixture using standard and two-stage mixing methods. They also measured their mechanical properties and performed microstructural analysis. However, the analysis of the influencing factor of fiber content was lacking. Moosa et al. [19] analyzed the mechanical properties and fracture energy of high-strength FRC. Meanwhile, the study on the influence of water–binder ratio was more in depth, while that on the influence factor of fiber content was lacking. Islam et al. [20] showed that the workability of concrete decreased with the increase in fiber length. However, studies on the influence factor of fiber type are lacking. Rashed et al. [21], based on previous studies, suggested that the extrusion process would preferentially align fibers parallel to tensile stresses, thereby enhancing the concrete's fracture properties. However, the analysis of its compression performance was lacking. Savio et al. [22] examined the influences of polypropylene fiber volume, slenderness ratio, and reinforcement indexes on the cracking performance of concrete, including toughness and residual strength. But there was a lack of studies on axial compressive performance. Rodrigues et al. [23] evaluated the stiffness, damage expansion behavior, and crack development of samples of polyvinyl alcohol FRC, polypropylene FRC, and plain concrete. The properties of the three materials were compared under three-point bending cycle and quasi-static test. Meanwhile, the interaction between the two fibers was not analyzed. On the basis of literature data, Chen et al. [24] quantitatively analyzed the change law of concrete creep with time and steel fiber content, but the compressive resistance performance was not described in detail.

The aforementioned results mainly focused on the crack resistance, bending resistance, and fracture properties of different types of FRC. However, the study on the compressive performance, the mixing effects of different fibers, the influence of fiber content, and the mechanical properties of fibers are not detailed enough. In this study, a constitutive model is formulated, and an axial compressive test is conducted, utilizing the compressive strength of various types of fiber concrete. The study examines the effect of both the type and quantity of fiber added to FRC using three different methods of fiber incorporation. This exploration serves as a foundational step for optimizing and testing FRC.

The rest of this study is organized as follows. Section 3 describes the design of compressive test scheme and material parameters of FRC. In Section 4, the improvement degree of the two fibers on the compressive properties of concrete is obtained through the analysis of the test results. By constructing the stress-strain constitutive relationship, the finite element software is simulated and compared with the test values to verify the accuracy of the model. The last section summarizes this study and gives some conclusions.

3. Methodology

3.1 Test scheme

To ascertain the ideal content that maximizes the performance of fiber materials in concrete, conducting fundamental mechanical tests on Fiber Reinforced Concrete (FRC) blocks becomes imperative. As per Wang et al. [25], the addition of short glass fibers to concrete can diminish its bending strength when the fiber content surpasses an optimal level. Hence, it is recommended not to exceed a 1% fiber content, as an excess of fibers might cause clustering during the concrete mixing and vibrating processes. Consequently, this study opts for three fiber mixing rates—0.3%, 0.6%, and 0.9%-for experimental analysis.

The article designs a total of 58 sets, amounting to 174 prism blocks (58 × 3). This includes 87 compression test specimens measuring 150 mm × 150 mm × 300 mm, 29 sets of 87 flexural test modulus of elasticity test specimens of the same size, and 57 flexural test specimens measuring 100 mm × 100 mm × 400 mm. Each type of tests also includes a control group consisting of 1set or 3 plain concrete blocks. The overall experimental scheme is presented in Table 1. The mechanical properties of the staple fiber materials used in this study are shown in Table 2.

The experiment adheres to the guidelines outlined in the Standard Test Methods for Mechanical Properties of Ordinary Concrete [26]. The axial compression test is executed using a 1000 kN testing apparatus at Beijing University of Technology, depicted in Figure 1. This test aims to derive the entire stress-strain curve and ascertain the axial compressive strength of the concrete blocks. The loading procedure is stress-controlled, involving the placement of the specimen onto the machine's platform and the gradual application of an axial load at a rate of 0.5MPa/s until the specimen reaches failure.

Table 1. Test plan

Fiber addition rate	C	A	CA
0.3%	3	3	3
0.6%	3	3	3
0.9%	3	3	3

Note: C stands for carbon fiber, A stands for aramid fiber, CA stands for hybrid fiber of both, the following are the same.

Table 2. Mechanical properties of chopped fibers

Fiber type	Density kg/m^3	Tensile strength MPa	Tensile modulus GPa	Elongation %	Fiber diameter μm	Cut length mm
C	1750	3530	240	1.5	8	12
A	1440	3150	80	3.6	12	12

Fig. 1. Axial compression test instrument

3.2 Constitutive Model

The complete compressive curve serves as the primary material foundation for studying and analyzing the mechanical properties of structures and components in graphical constitutive relations. Therefore, it becomes crucial to develop a suitable mathematical model for this specific purpose. Considering the distinct characteristics of the compressive stress-strain curve of FRC, this study introduces three reference calculation models:

Xu et al. [27] proposed that the stress – strain curve obtained from the test block test should be represented by dimensionless coordinates.

$$\begin{cases} \overline{x} = \varepsilon/\varepsilon_u \\ \overline{y} = \sigma/\sigma_u \end{cases} \tag{1}$$

where and represent the peak strain and stress values of the test block, respectively.

Plot a curve with peak coordinates (1,1), as shown in Figure 2.

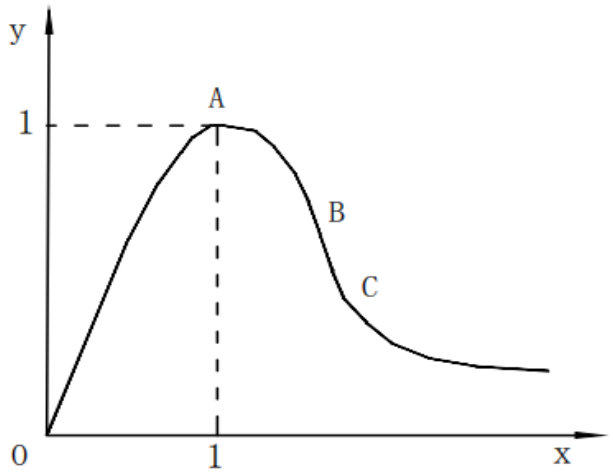

Fig. 2. Dimensionless Stress-Strain Complete Curve of Fiber Reinforced Concrete under Uniaxial Compression.

According to the analysis of constitutive curves summarized by Guo et al. [28], a segmented curve was more effective in describing the trend of stress – strain development. The equation was represented as follows:

$$\begin{cases} y = ax + (3-2a)x^2 + (a-2)x^3 & (0 \le x \le 1) \\ y = \dfrac{x}{b(x-1)^2 + x} & (x > 1) \end{cases} \tag{2}$$

where a and b are unknown parameters.

The curve equation proposed by Guo et al. [29] was represented as follows:

$$y = \frac{x}{a_1 + a_2 x + a_3 x^2 + a_4 x^3} \tag{3}$$

where a_1, a_2, a_3, and a_4 are unknown parameters.

In the rising part of the curve, namely, the OA segment, the slope monotonically decreases until point A, where the slope becomes zero. Based on this condition, Equation (2.3) results in: $a_2 = 0, a_3 = 0, a_4 = 2a_1 - 1$. The study in Reference [5] suggested that the rising and falling segments of the curve were relatively independent, with continuity at Point A being the only requirement. Additionally, according to References [4-7], Equation (2.2) provided a more accurate description of the characteristics of the falling segment of the curve. Therefore, the descending part of the curve adopted the formula for x > 1 from Equation (2.2), which could be proven to meet all the requirements of the curve. The curve could be represented as follows:

$$\begin{cases} y = \dfrac{x}{a_1 + (2-3a_1)x^2 + (2a_1 - 1)x^3} & (0 \le x \le 1) \\ y = \dfrac{x}{b(x-1)^2 + x} & (x > 1) \end{cases} \tag{4}$$

where a_1 and b are unknown parameters.

The curve equation suggested by Deng et al. [30] was expressed as follows:

$$y = \frac{a_1 x + (a_2 - 1)x^2}{1 + (a_1 - 2)x + a_2 x^2} \tag{5}$$

where a_1 and a_2 are unknown parameters.

Because the curve exhibited a monotonically decreasing slope within the (0, 1) interval, we set a_2 to be equal to 0 to simplify calculations. After computation, in this scenario, the second derivative d^2y/dx^2 consistently remains less than 0, which fulfills the curve's requirements. Consequently, the descending segment continues to use the formula from section x > 1, resulting in the following representation of the curve:

$$\begin{cases} y = \dfrac{a_1 x - x^2}{1 + (a_1 - 2)x} & (0 \le x \le 1) \\ y = \dfrac{x}{b(x-1)^2 + x} & (x > 1) \end{cases} \tag{6}$$

where a_1 and b are unknown parameters.

3.3 Finite Element Simulation

The comprehensive simulation of the FRC beam is conducted utilizing three-dimensional eight-node hexahedral solid elements, a methodology extensively documented in existing literature. The fibers integrated into the concrete were represented using beam elements, detailing their force characteristics along the length and width directions, while disregarding the normal forces acting on the fibers. Precisely, this simulation approach was accomplished through the utilization of a Python programming plugin. This plugin created uniformly and randomly distributed fiber elements in space, generating a py file recognizable by ABAQUS software. This script was then run within the established experimental beam model. The mechanical properties of the fiber material were defined, attributes were assigned to the fiber beam elements, and the mesh was divided. Subsequently, the generated fiber components were connected to the FRC beam model as embedded regions.

4. Result Analysis and Discussion

According to the axial compressive strength, the strength variation law and stress–strain curve of concrete test block under different fiber types and contents can be obtained. The experiment was completed in the laboratory of Beijing University of Technology.

4.1 Axial Compression Test

The axial compressive strength of FRC can be obtained through the compressive test. These tests cannot only obtain the change trend of concrete strength under different fiber addition rates, so as to determine the optimal addition rate, but can also determine the accuracy of the calculation formula of compressive strength of FRC stipulated in existing norms for hybrid FRC. It provides the basis for the subsequent calculation of the bearing capacity of fiber partially prestressed concrete beams.

In the experiment, every group comprises three samples, and the one that aligns closest with the average strength and displays typical failure patterns is selected for analysis, as depicted in Figure 3.

In the test block with 0.3% fiber content, although the carbon fiber test block has cracking phenomenon, the concrete does not fall off, and the rest of the cracks are dense without any appearance of through cracks. There are many small diagonal cracks on the surface of the aramid fiber test block, and there is no sign of concrete falling off. The cracks of hybrid fiber test block develop vertically, and some concrete bulges but do not fall.

In 0.6% fiber content concrete test block, the brittleness of concrete is slightly improved with the increase of carbon fiber content. The cracks of aramid fiber test block are more dense and interlaced, and the concrete does not spalling. The hybrid fiber test block has cracks at the end and develops downward. Except for the main cracks, the other cracks are short and thin, and the concrete does not swell or spalling.

In the concrete test block with 0.9% fiber content, the crack width of the carbon fiber test block is larger, but the concrete does not fall because of the connection of internal fibers. There is a main oblique crack from the bottom to the middle span of the aramid fiber test block, and many fine cracks can be seen on the surface. The hybrid fiber test block protrudes at the middle 1/2 of the surface, and a single fiber filament crosses the crack, limiting the concrete's fall.

From the analysis of the failure phenomenon of the test block, when the fiber content is small, the compressive strength is slightly improved, and the brittleness property is greatly improved. Upon increasing the content to 0.6%, the compressive strength demonstrates the most significant enhancement, alongside an improvement in ductility compared to the block doped with 0.3%. However, the compressive strength of the test blocks experiences a decline when the content is further escalated to 0.9%. According to the study of Wang et al. [31], adding an appropriate amount of basalt fiber can effectively improve the ultimate bearing capacity of short concrete columns. It can be analyzed that too many fibers may cause clumping, forming weak points and leading to brittleness of test blocks. According to the analysis, 0.6% is the best choice for the three fiber contents.

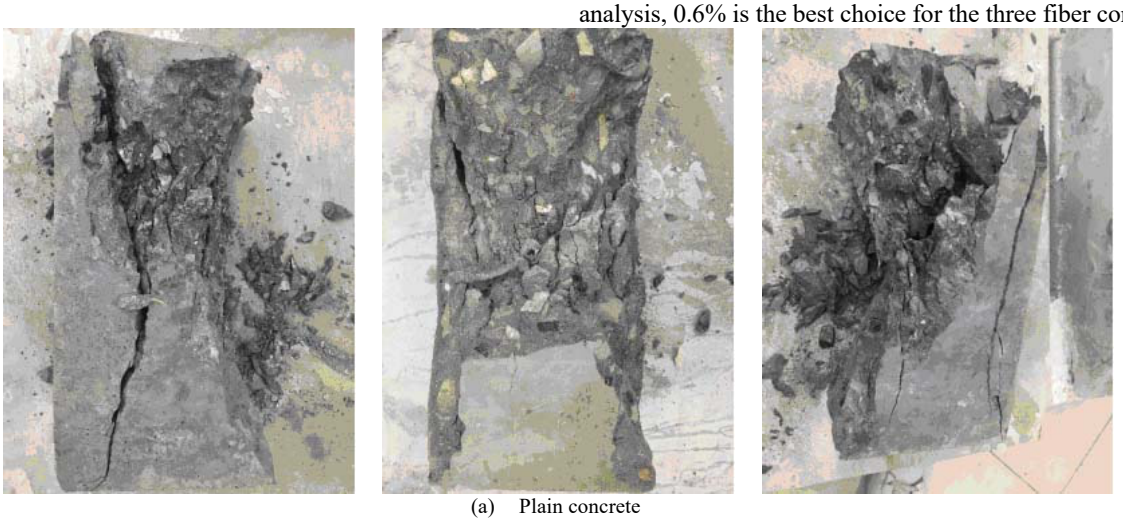

(a) Plain concrete

0.3% fiber content　　0.6% fiber content　　0.9% fiber content

(b) carbon fiber reinforced concrete

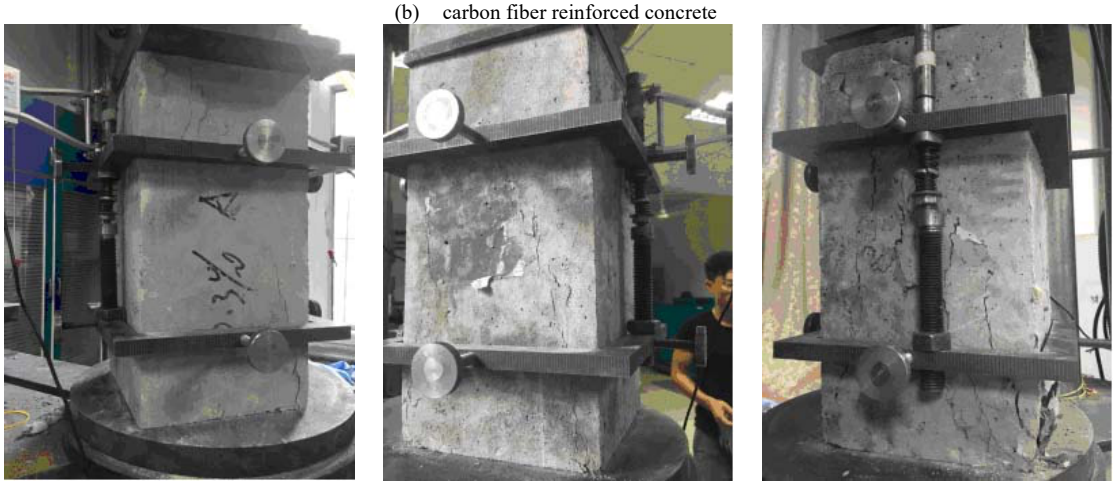

0.3% fiber content　　0.6% fiber content　　0.9% fiber content

(c) aramid fiber reinforced concrete

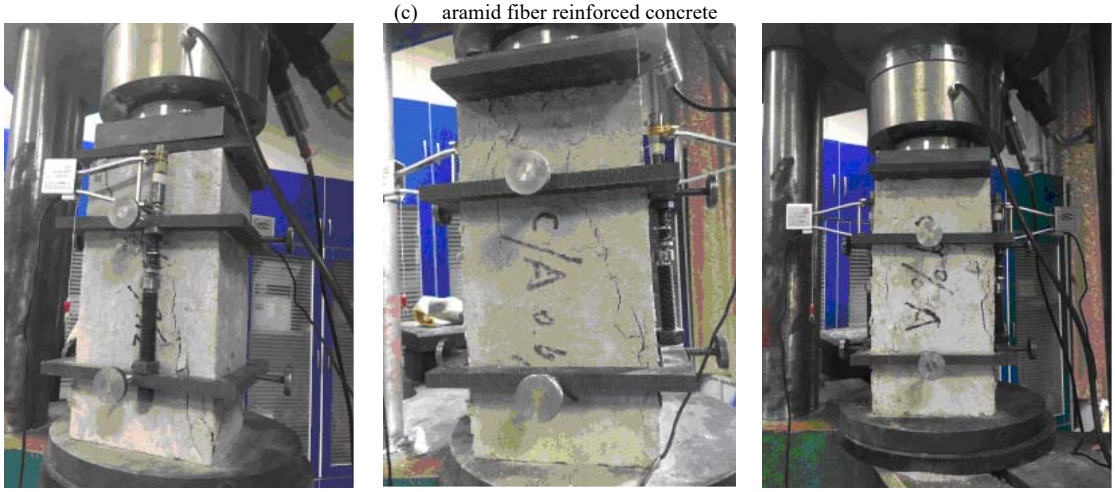

0.3% fiber content　　0.6% fiber content　　0.9% fiber content

(d) Hybrid fiber reinforced concrete

Fig. 3. Specimen failure diagram

4.2 Compressive strength results

The experimental system automatically collected data, as shown in Table 3.

This can be seen directly from the above table. With increasing fiber content in concrete, there is a general trend of initial increase followed by a decrease in compressive strength. When the fiber content is low, it does not significantly affect strength, showing little to no change. However, with a fiber content of 0.6%, the compressive strength of concrete with aramid fibers increased the most. At a fiber content of 0.9%, the excessive amount of fiber becomes challenging to uniformly disperse. This abundance of fibers during the mixing process tends to clump together, creating vulnerable spots within the concrete. Consequently, the compressive strength gradually decreases with the escalating content. However, when aramid fiber and carbon fiber are blended into the concrete test block, they exhibit a synergistic effect, leveraging each other's strengths. This synergy maximizes the advantages of both fibers, resulting in a substantial enhancement of the concrete's compressive strength.

Table.3. Average axial compressive strength of concrete test block $f_{ck}(N/mm^2)$

Fiber type	Fiber addition rate（%）			
	0	0.3	0.6	0.9
C	40.4	39.3	41.9	37.8
A		39.5	44.3	36.9
CA		39.4	42.4	40.5

4.3 Complete Stress-Strain Curve

Throughout the compression test until failure, the system gathered comprehensive data detailing variations in stress and strain. To provide a clearer depiction of the differences in the descending segment of the curve during the compression process of the test block, a specific strain range from 0 to 0.007 is isolated for analysis. Figure 4 illustrates the entire curve of plain concrete for reference.

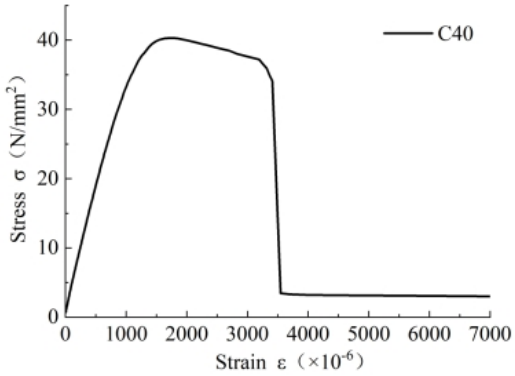

Fig. 4. Full stress-strain curve of plain concrete

The curve in Figure 4 shows that the plain concrete test block has obvious brittleness characteristics. After the load reaches the maximum value, the curve drops abruptly, the test block cracks instantaneously, declaring failure, and the residual bearing capacity is basically zero.

Upon comparing the curves of the test block at various contents, it's evident that lower content results in reduced strength and increased strain. As the content increases, stress elevates while strain decreases. However, when the content surpasses 0.6%, the stress of the test block diminishes to varying extents, with some exhibiting brittle failure. Analysis indicates that at lower dosages, the limited number of fibers hampers their full utilization. Conversely, excessive content leads to an abundance of fibers that cannot be effectively dispersed during the mixing process, causing fiber clumping and the formation of weak spots in the concrete. This situation results in a phenomenon of stress decline and eventual brittle failure.

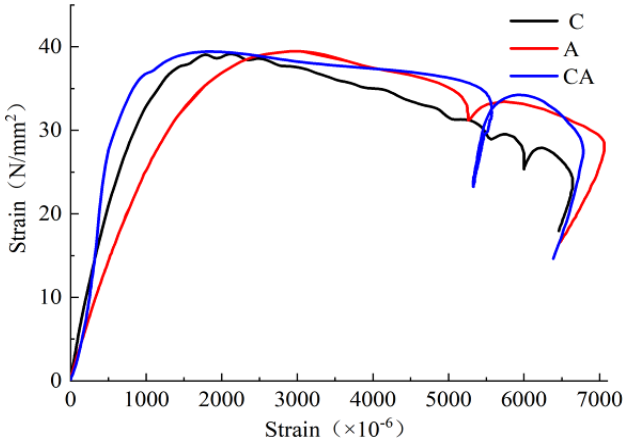

(a) 0.3% fiber content

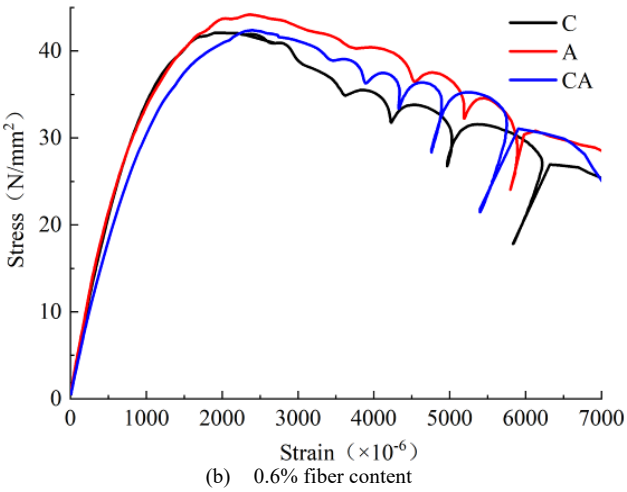

(b) 0.6% fiber content

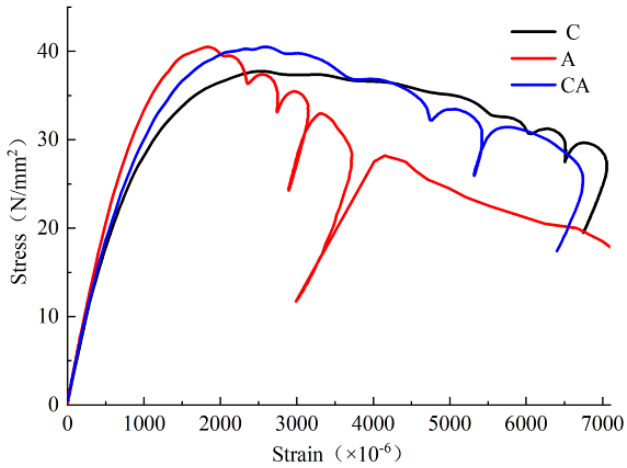

(c) 0.9% fiber content

Fig. 5. Comparison of stress-strain curves of different fiber types

Based on the study of strength, compressive strength and stress–strain curve of FRC. It is concluded that the mixture of 0.6% fiber is the best choice, and the economy is better.

4.4 Model Parameter Study

Based on the experimental results, the optimal fiber content is determined to be 0.6%. Table 4 lists the characteristic parameters of the complete curve for contents of 0.3%, 0.6%, and 0.9%. Due to the restraining effect of fibers, the concrete's crack initiation load is increased, significantly lengthening the linear portion of the curve and slowing down the appearance and development of cracks. After reaching peak load, the descending part of the curve is relatively slow, and the samples retain some residual strength. These characteristics indicate that the parameters of the complete curve model for FRC differ from those of regular concrete.

As the fiber content increases, the parameter "a" in the ascending segment of the uniaxial compression stress-strain curve steadily rises, while the parameter "b" in the descending segment gradually decreases. This trend results in the gradual flattening of both the rising and falling sections of the curve. Consequently, the area beneath the curve progressively enlarges with the increasing fiber

content. This increase in area signifies higher energy absorption during the compressive failure process of the specimen, ultimately enhancing the compressive toughness of the specimen. Based on the three constitutive models in Section 3.3, this study uses the least square method to fit the test data obtained from the three fiber content test blocks, and the parameters of the model are shown in Table 5.

Table 4. Test block curve feature point parameters

Fiber type	Adding rate	P_u / kN	σ_u / MPa	$\sigma_{0.5}$ / MPa	ε_u /10^{-3}	$\varepsilon_{0.85}$ /10^{-3}	$\varepsilon_{0.5}$ /10^{-3}
C	0.3%	911	39.5	18.75	2.03	4.31	5.61
A		920	38.9	19.45	1.63	2.47	6.33
CA		914	40.6	20.30	2.46	4.30	5.44
C	0.6%	943	39.9	19.95	1.90	3.55	6.01
A		997	39.3	19.15	2.38	4.47	8.35
CA		954	40.2	20.10	2.40	4.32	7.43
C	0.9%	873	38.8	19.40	2.41	4.16	5.62
A		887	39.4	19.70	2.55	4.83	7.36
CA		927	39.4	19.70	2.17	3.65	6.39

Note: Pu represents the peak load, σ_u the peak stress, $\sigma_{0.5}$ the stress when the load drops to 50% of the peak load, ε_u the peak strain, and $\varepsilon_{0.85}$, $\varepsilon_{0.5}$ the strains corresponding to 85% and 50% of the peak load, respectively.

Table 5. Parameters of fiber reinforced concrete test block compression constitutive model

Fiber type	Adding rate	The Guo Zhenhai model		The Saenz model		The Sargin model		Descent stage	
		a	R^2	a_1	R^2	a_1	R^2	b	R^2
C	0.3%	2.42	0.999	0.47	0.998	2.47	0.999	0.30	0.888
A		2.29	0.999	0.49	0.997	2.32	0.999	0.17	0.930
CA		2.73	0.999	0.42	0.998	2.90	0.999	0.34	0.989
C	0.6%	2.30	0.999	0.50	0.998	2.33	0.999	0.35	0.977
A		2.56	0.999	0.45	0.999	2.66	0.998	0.60	0.908
CA		2.41	0.999	0.47	0.997	2.47	0.999	0.81	0.924
C	0.9%	2.30	0.999	0.38	0.996	3.35	0.999	0.41	0.968
A		2.75	0.999	0.42	0.998	2.95	0.999	0.41	0.988
CA		2.55	0.999	0.45	0.999	2.61	0.998	0.57	0.979

Note: R^2 is the correlation coefficient, and all data in the table are averages.

The data indicates that all three model formulas exhibit a high level of accuracy in fitting the ascending segment of the stress–strain curve for the three types of fibers. The Guo Zhenhai and Deng Mingke model parameter values demonstrate relatively similar trends. However, there is a slight reduction in the accuracy of fitting observed in the descending segment. Analysis indicates that the three fibers chosen in this study exhibit good ductility. After reaching the ultimate load, the test block experiences a relatively gradual decrease in load, accompanied by an increase in strain, resulting in a more comprehensive curve. The fitting outcomes of the curves at the three different contents suggest that this model exhibits stable robustness.

The stress-strain full curve fitting of different fiber types at the addition rate of three fibers is shown in Figure 6 (Guo Zhenhai constitutive model is selected).

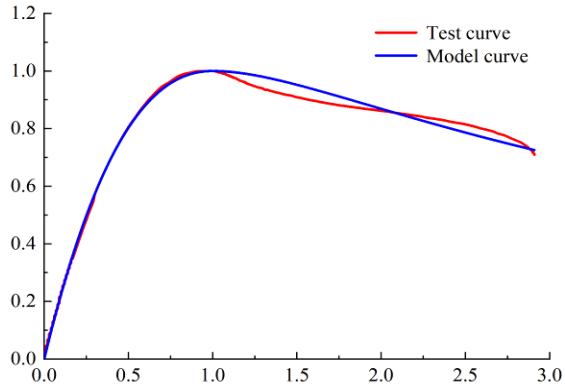

(1) Carbon fiber

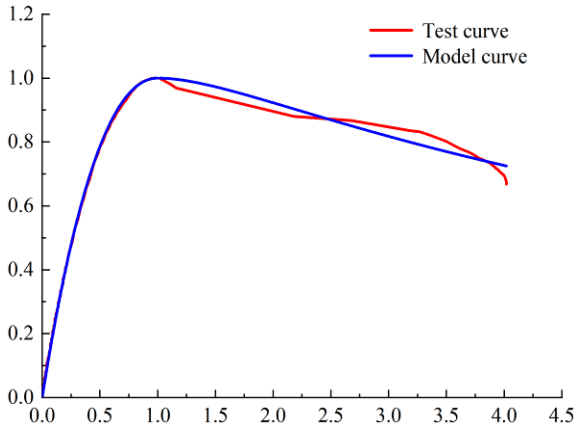

(2) Aramid fiber

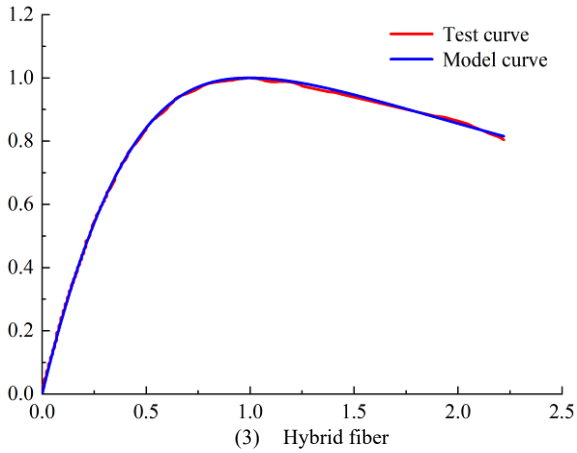

(3) Hybrid fiber

(a) 0.30% fiber content

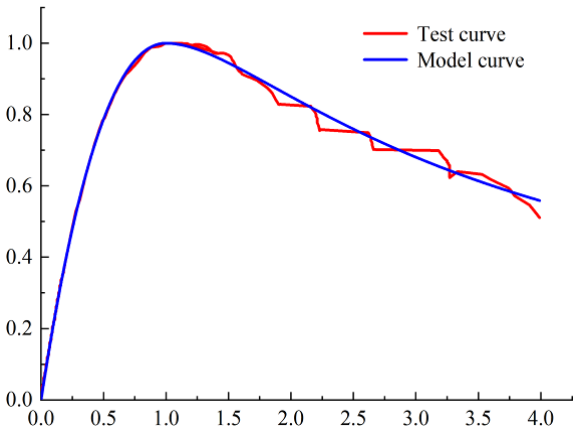

(1) Carbon fiber

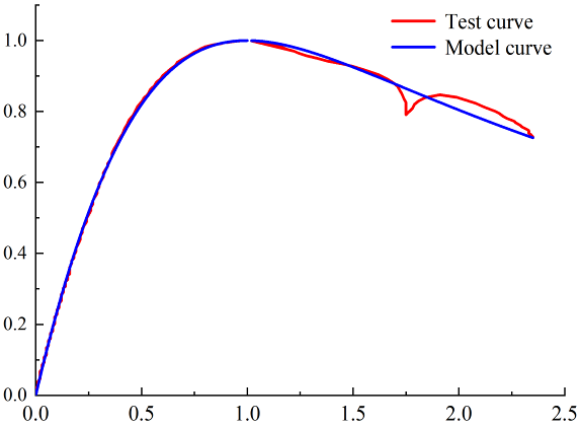

(2) Aramid fiber

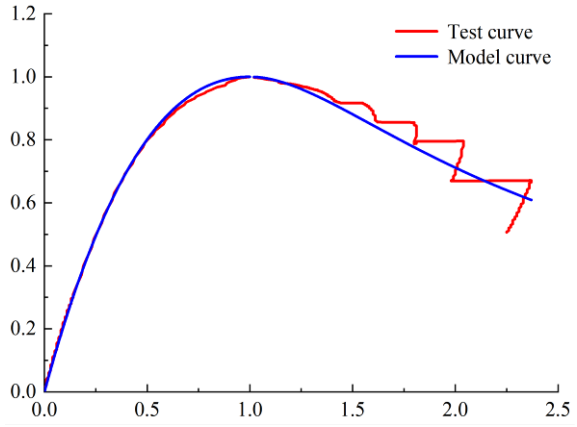

(3) Hybrid fiber

(b) 0.60% fiber content

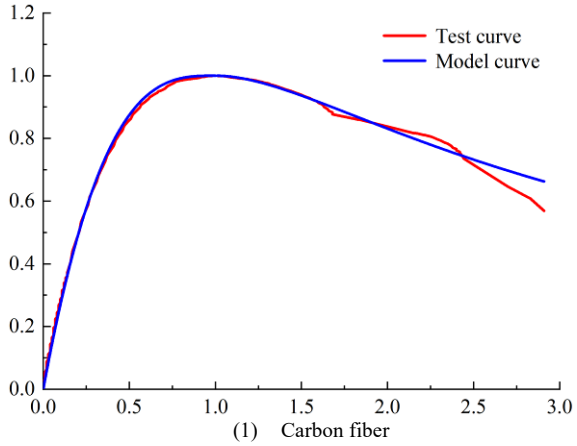

(1) Carbon fiber

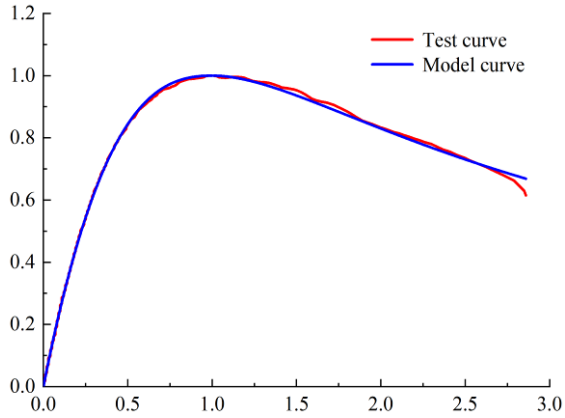

(2) Aramid fiber

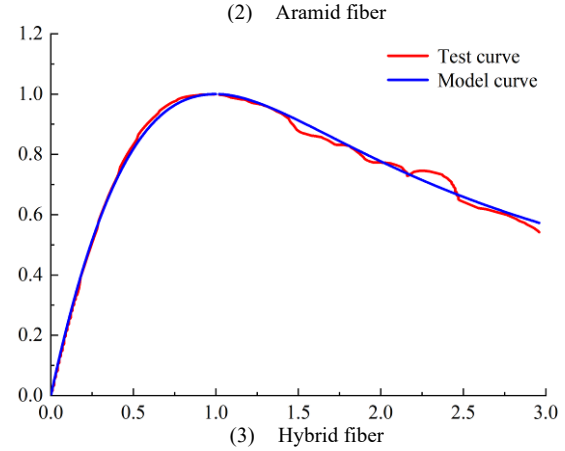

(3) Hybrid fiber

(c) 0.90% fiber content

Fig. 6. Constitutive models of fiber reinforced concrete with different fiber types in three kinds of mixtures

4.5 Numerical simulation results and comparison

The simulated block size uses a prism of 150 mm × 150 mm × 300 mm. The concrete uses hexahedral C3D8R elements, with a global size of 15 mm for mesh division. The fibers use a beam element model, with a global size of 6 mm for mesh division. Feature points are selected on the top surface of the prism and set to couple with the top surface, and the loading method is displacement loading.

4.5.1 Stress-Strain Curve

In the results file, the stress-strain data of the 0.6% fiber content concrete model sample is extracted and plotted into a curve, which is then compared with the experimental curve, as shown in Figure 7.

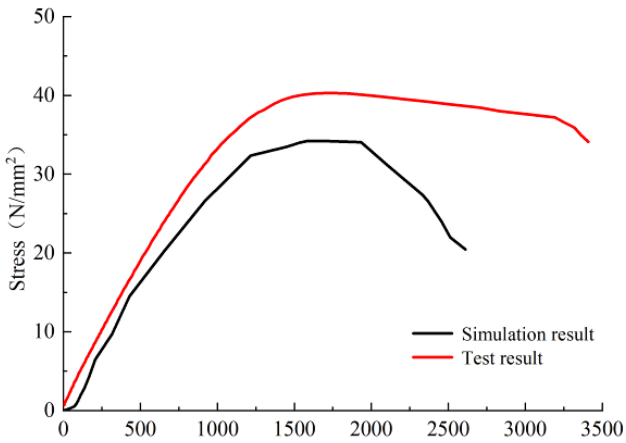

(a) Ordinary concrete

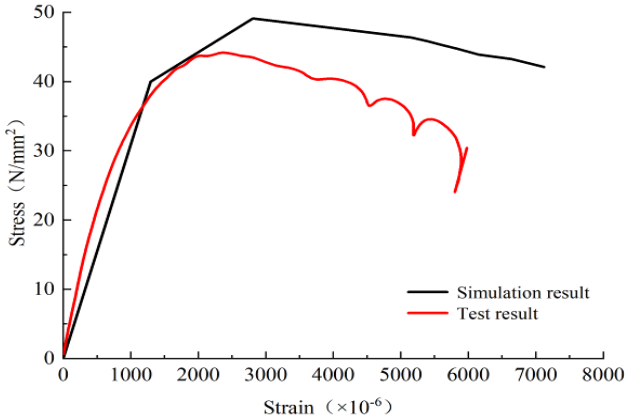

(b) Carbon fiber reinforced concrete

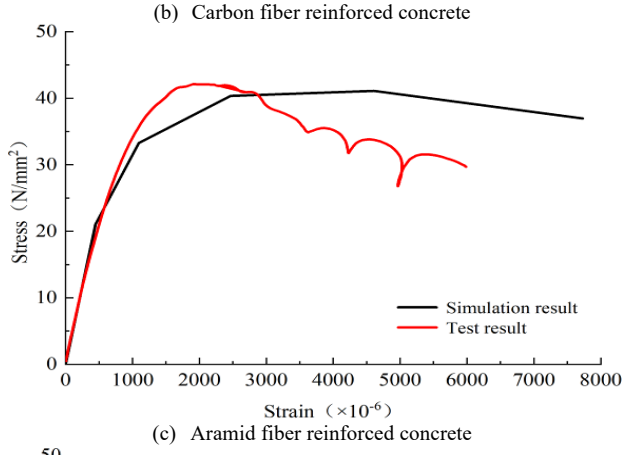

(c) Aramid fiber reinforced concrete

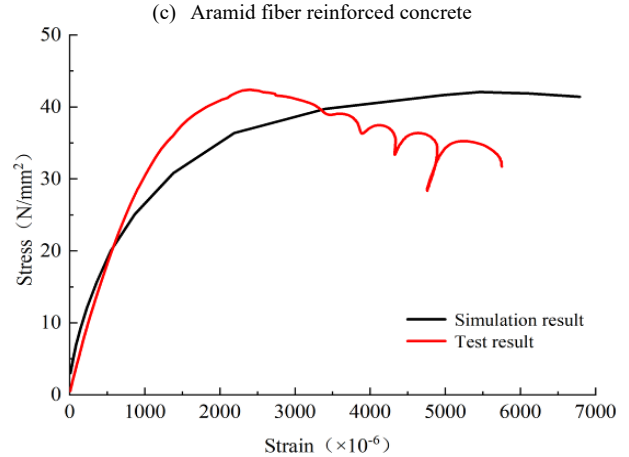

(d) Hybrid fiber reinforced concrete

Fig. 7. Stress-strain curve of fiber reinforced concrete test block

The curve shows that the simulation results and the experimental results have basically the same trend. After reaching the ultimate compressive strength, the stress of the ordinary concrete samples drops quickly, showing brittleness. Overall, the simulation of the stress–strain constitutive relationship of FRC under compression is slightly different in the softening segment compared to the experimental results, with the numerical simulation results declining more slowly. From the numerical simulation, the aramid fibers in the FRC samples have the most significant effect on improving the brittleness of the concrete. Additionally, in the simulation, the compressive strength of the carbon FRC samples is higher than the experimental values. According to Kan et al. [32], carbon fibers have a negative effect on the absorption of moisture in concrete. It is believed that in actual operations, the hydrophilicity of carbon fibers may cause them to clump during mixing, thus negatively affecting the experimental strength.

4.5.2 Strength Comparison Results

The compressive strength results of the model samples are compared with the experimental values, as shown in Table 6.

Table. 6. Axial compressive strength of concrete specimen (unit: MPa)

Specimen type	Experimental value	Simulated value
Ordinary concrete	40.4	34.22
Carbon fiber reinforced concrete	44.2	49.12
Aramid fiber reinforced concrete	41.9	41.10
Hybrid fiber reinforced concrete	42.4	42.07

The simulation results of ordinary concrete data are small, whereas carbon FRC data are large. However, the error is kept within 15%, indicating high accuracy. As proven, the method can be used in the simulation study of test beams.

5. Conclusions

To explore the mechanical properties of FRC mixed with carbon fiber, aramid fiber and the hybrid fibers, numerical simulation technology and experimental research were combined in this study. The compressive strength and stress–strain curves of concrete test blocks with different fiber types and content were studied. The finite element numerical simulation of FRC was carried out on the basis of the constitutive model. The following conclusions could be drawn:

(1) In the axial compression test, multiple vertical cracks appear on the surface of the FRC test block when it is compressed, and the concrete is finally damaged because it is fractured and loses its bearing capacity. The test block always maintains integrity during the process. The compressive strength of FRC test block increases first and then decreases with the increase in fiber volume addition rate from 0%–0.9%. When the fiber volume addition rate is 0.6%, the improvement effect is evident, and the maximum increase rate is approximately 10%. The improvement of compressive strength of aramid FRC is the most evident, followed by hybrid fiber.

(2) Based on the above experimental results, the optimal fiber content is preliminarily determined to be 0.6%. Based on the concrete constitutive model proposed by Guo Zhenhai and others, the complete stress–strain curves of FRC at 0.3%, 0.6%, and 0.9% contents are fitted, consistent with the experimental results. According to the fitted constitutive, a model is established using finite element software and compared with experimental values, thereby proving the model's high accuracy.

In this study, combining laboratory experiments with finite element simulation, carbon fiber, and aramid fiber, as well as their mixture are proposed to improve concrete. The stress–strain constitutive model established can accurately describe the stress process and performance of FRC. It can provide theoretical reference for the promotion and application of FRC. Due to the lack of consideration of the influence of the strength grade of concrete materials, the data from concrete with various strength grades will be integrated with this model and adjusted in the future work. This integration aims to refine and enhance the model, enabling a more precise understanding of the effect patterns specific to fiber concrete across different strength grades.

Acknowledgements

This work was supported by the Doctoral Research Fund (BKY-2020-27), the Science Research Project of Hebei Education Department (ZC2023175), the Construction of Scientific and Technological Research Project by Hebei Department of Housing and Urban-Rural Development (2023-2156)

References

[1] H. Huang, Y. J. Yuan, W. Zhang, and L. Zhu, "Property assessment of high-performance concrete containing three types of fibers," *Int. J. Concr. Struct. Mater.*, vol. 15, no. 1, Dec. 2021, Art. No. 39.

[2] B. Han, L. Zhang, C. Zhang, Y. Wang, X. Yu, and J. Ou, "Reinforcement effect and mechanism of carbon fibers to mechanical and electrically conductive properties of cement-based materials," *Constr. Build. Mater.,* vol. 125, pp. 479–486, Oct. 2016.

[3] P. Xu, J. Y. Ma, Y. H. Ding, and M. X. Zhang, "Influences of Steel Fiber Content on Size Effect of the Fracture Energy of High-Strength Concrete," *KSCE J. Civ. Eng.*, vol. 25, no. 3, pp. 948-959, Mar. 2021.

[4] W. Chen, J. Wang, K. Zhang, J. Chen, G. J. Liu, and Z. Y. Zhu, "Anti-crack Performance of Reinforced Concrete Beams Strengthened by Basalt Fiber," *J. Mater. Sci. Eng.*, vol. 35, no. 1, pp. 144-148, Feb. 2017.

[5] S. Q. Zhao, Q. L.You, J. Z. Li, J. Yin, and Z. Y. Huang, "Analysis of toughening and cracking resistance effect of modified polyester fiber on airport cement concrete," *Mater. guide*, to be published. Accessed: Aug. 23, 2023. doi: 10.11896/cldb.23030172. [Online]. Available: http://kns.cnki.net/kcms/detail/50.1078.TB.20230824.1442.016

[6] Y. C. Huang, D. Y. Gao, H. T. Zhu, D. Fang, and C. Ding, "Probability distribution and value suggestion of steel fiber influence coefficient of reinforced concrete beam in tensile zone,". *J. Basic Sci. Eng.*, to be published. Accessed: Oct. 13, 2023. [Online.] Available: https://link.cnki.net/urlid/11.3242.TB.20231011.1225.002

[7] Y. Xu, Y. Fan, Q. Y. Wang, and Z. Y. Zhang, "Test and numerical analysis of fracture toughness of polypropylene fiber reinforced concrete," *J. Jilin Univ. (Eng. Tech. Ed.)*, to be published. Accessed: Jun. 13, 2023. doi: 10.13229/j.cnki.jdxbgxb.20221551. [Online]. Available: https://doi.org/10.13229/j.cnki.jdxbgxb.20221551

[8] A. A. Sadoon, M. A. Al-Shugaa, M. K. Rahman, A. Al-Fakih, and M. A. Al-Osta, "Enhancing unreinforced masonry wall resilience through nano-silica modified steel fiber reinforced mortar: A study on in-plane cyclic loading," *Case Stud. Constr. Mater.*, vol. 19, Dec. 2023, Art. no. e02358.

[9] J. F. Guan, M. Lu, H. Wang, X. H. Yao, L. L. Li, and M. Zhang, "Simultaneously determining fracture toughness and tensile strength of steel fiber high- strength concrete," *Eng. Mech.*, vol. 40, no. 3, pp. 65-77, Mar. 2023.

[10] L. Jin, L. K. Jia, and R. B. Zhang, "Microscopic numerical study on fracture behavior of steel fiber reinforced concrete at low temperature," *Eng. Mech.*, vol. 40, no. S1, pp. 200-206, Jun. 2023.

[11] Z. G. Zhang, *et al*, "Experimental and numerical evaluation for tunnel structural stability of fiber concrete lining with different crack features under train load," *Eng. Fail. Anal.*, vol. 153, Nov. 2023, Art. no. 107530.

[12] X. F. Zhang, S. Z. Wang, Y. L. Pang, Z. J. Yu, and X. W. Wei, "Effect of aggregate size and fiber length on mechanical properties of basalt fiber concrete," *Water Resour. Power*, vol. 41, no. 11, pp. 160-164, Nov. 2023.

[13] C. G. Zhao, Z. Y. Wang, Z. Y. Zhu, Q. Y. Guo, X. R. Wu, and R. D. Zhao, "Research on different types of fiber reinforced concrete in recent years: An overview," *Constr. Build. Mater*., vol. 365, Feb. 2023, Art. no. 130075.

[14] X. Liu, Q. H. Sun, Y. Yuan, and L. Taerwe, "Comparison of the structural behavior of reinforced concrete tunnel segments with steel fiber and synthetic fiber addition," *Tunn. Undergr. Sp. Tech.*, vol. 103, Sep. 2020, Art. no. 103506.

[15] D. Y. Wang, J. S. Qi, G. Y. Cui, Y. L. Yang, and J. Chang, "Model Test on Bearing Characteristics of Basalt Fiber-Reinforced Concrete Lining," *Adv. Mater. Sci. Eng.*, vol. 2020, Mar. 2020, Art. no. 3891343.

[16] F. Y. Li, Y. X. Cui, C. Y. Cao, and P. F. Wu, "Experimental study of the tensile and flexural mechanical properties of directionally distributed steel fibre-reinforced concrete," *P. I. Mech. Eng. L-J. Mat.*, vol. 233, no. 9, pp. 1721-1732, Sep. 2019.

[17] S. Guler and Z. F. Akbulut, "The coupling effect of silica fume and basalt fibers on workability and residual strength capacities of traditional concrete before and after freeze–thaw cycles," *Arch. Civ. Mech. Eng.*, vol. 23, no. 3, Jun. 2023, Art. no. 173.

[18] O. Onur and O. Nilufer, "Implementation of two-stage mixing approach to improve the performance of fiber reinforced concrete for sustainable construction," *Constr. Build. Mater.*, vol. 409, Dec. 2023, Art. no. 133870.

[19] M. Moosa, N. A. Oveys, and B. Hamid, "The fracture energy and mechanical properties of high-strength concrete containing polyolefin macro-fibres," *Eur. J. Environ. Civ. En.*, vol. 27, no. 13, pp. 3834-3848, Oct. 2023.

[20] T. Islam, M. Safiuddin, A. R. Roman, B. Chakma, and A. Al Maroof, "Mechanical Properties of PVC Fiber-Reinforced Concrete—Effects of Fiber Content and Length," *Buildings-Basel*, vol. 13, no. 10, Oct. 2023, Art. no. 2666.

[21] R. Alarrak, B. Jeon, and A. S. Brand, "Fracture properties of extruded fiber-reinforced mortar with preferentially aligned fibers," *Constr. Build. Mater.*, vol. 403, Nov. 2023, Art. no. 133022.

[22] A. Del Savio, D. Esquivel, and G. M. Landeo, "Post-Cracking Properties of Concrete Reinforced with Polypropylene Fibers through the Barcelona Test," *Polymers-Basel*, vol. 15, no. 18, Sep. 2023, Art. no. 3718.

[23] F. R. De Souza, V. A. Lima, N. R. D. Cerqueira, D. C. T. Cardoso, and F. D. Silva, "Flexural behavior of PVA and PP fiber-reinforced concrete under cyclic loading," *J. Braz. Soc. Mech. Sci.*, vol. 45, no. 9, Sep. 2023, Art. no. 472.

[24] C. Chen, F. Y. Gong, X. Y. Zhao, and B. Zeng, "Effects of fiber and admixture on creep of concrete are summarized," *Concrete*, vol. 5, pp. 85-91+95, May. 2023.

[25] W. C. Wang, H. Y. Wang, K. H. Chang, and S. Y. Wang, "Effect of high temperature on the strength and thermal conductivity of glass fiber concrete," *Constr. Build. Mater.*, vol. 245, Jun. 2020, Art. no. 118387.

[26] *Standard of Test Method for Mechanical Properties of Ordinary Concrete* GB/T50081-2002. Beijing, China Academy of Building Research, 2007.

[27] L. H. Xu, B. Li, Y. Chi, B. Huang, C. N. Li, and Y. C. Shi, "Experimental investigation on stress-strain relation of steel-polypropylene hybrid fiber reinforced concrete subjected to uniaxial cyclic compression," *J. Build. Struct.*, vol. 39, no. 4, pp. 140-152, Apr. 2018.

[28] Z. H. Guo, *Principle of Reinforced Concrete*. Beijing, Beijing, China: TU Press, 1999.

[29] Z. H. Guo, *Strength and Deformation of Concrete*. Beijing, Beijing, China: TU Press, 1997.

[30] M. K. Deng, J. J. Pan, M. Qin, and H. B. Liu, "Study on uniaxial compression constitutive model of high ductility concrete," *J. Xi 'an Univ. Arch. Tech. (Nat. Sci. Ed.)*, vol. 48, no. 6, pp. 826-831, Dec. 2016.

[31] X. Wang, Y. Yang, R. Yang, and P. Liu, "Experimental Analysis of Bearing Capacity of Basalt Fiber Reinforced Concrete Short Columns under Axial Compression," *Coatings*, vol. 12, no. 5, May. 2022, Art. no. 654.

[32] M. B. Khan, *et al*, "Optimization of Fresh and Mechanical Characteristics of Carbon Fiber-Reinforced Concrete Composites Using Response Surface Technique," *Buildings-Basel*, vol. 13, no. 4, Apr. 2023, Art. no. 852.